Analytical Methods

ROYAL SOCIETY OF CHEMISTRY

PAPER

View Article Online
View Journal | View Issue

Cite this: *Anal. Methods*, 2025, **17**, 1790

Comparison between electrochemiluminescence of luminol and electrocatalysis by Prussian blue for the detection of hydrogen peroxide†

Isnaini Rahmawati, *[a] Andrea Fiorani, [b] Irkham, [c] Wulan Tri Wahyuni, [d] Ruri Agung Wahyuono,[e] Yasuaki Einaga [b] and Tribidasari A. Ivandini *[a]

Received 29th November 2024
Accepted 19th January 2025

DOI: 10.1039/d4ay02175d

rsc.li/methods

Electrochemiluminescence (ECL) of luminol and electrocatalysis by Prussian blue were compared for the selective detection of H_2O_2 at the boron-doped diamond (BDD) electrodes. The H_2O_2 detection was optimized by various parameters such as the applied potential at pH 7.4, which is a physiological value usually used for H_2O_2 detection in enzymatic reactions. At an optimum applied potential of +0.5 V, a linear increase in the ECL signals ($R^2 = 0.99$) was achieved for H_2O_2 concentrations ranging between 0 to 100 μM with an estimated limit of detection (LOD) of 2.59 μM. This LOD was better than that obtained with electrocatalysis measurements using the same electrode modified with Prussian blue. Furthermore, the interference study in the presence of glucose, Fe^{3+}, Cl^-, Ca^{2+}, CO_3^{2-}, Na^+, and F^- ions showed a comparable selectivity of the luminol ECL and PB-BDD electrochemical current. Nevertheless, the ECL method exhibited significant advantage in the high stability of its signal response.

Introduction

Hydrogen peroxide (H_2O_2) is an important species in biology and chemistry and has wide applications in environmental, pharmaceutical, clinical, and industrial research.[1–3] It is also known as a by-product of the reactions catalysed by many oxidase enzymes.[4] Therefore, the detection of H_2O_2 is important in biomedical and environmental applications. Various detection techniques for H_2O_2 have been established, including colorimetry,[5] titrations,[6] chemiluminescence,[7] and fluorescence.[8] However, these methods can be time-consuming and costly or offer low selectivity and sensitivity.[2,3] Nowadays, electrochemical detection of H_2O_2 is widely used and has become a promising method with some advantages, such as reasonable cost, high sensitivity, good selectivity, simple instrumentation, and short measurement times.[1,2,9]

In electrochemical systems, the electrode is an important component in determining the performance of the sensor. Accordingly, various electrodes have been studied in the electrochemical detection of H_2O_2 to improve the sensitivity and selectivity of the sensor.[1] In the last decades, boron-doped diamond (BDD) has been widely studied as an electrode in electrochemical detection owing to their outstanding characteristics, such as good stability and biocompatibility as well as a significantly wider potential window and lower background current compared to the conventional electrodes.[10–15] This wide potential window happens owing to the high overpotential of the oxygen and hydrogen evolution reactions, which may further allow more selective detection of many chemical species in aqueous electrolytes.[11,12] In addition, BDD provides high resistance for applications at extreme potentials.[12] These characteristics make BDD electrodes attractive for electrochemical sensor applications.

Unfortunately, carbon-based electrodes, including BDD, are not electroactive for oxidation or reduction of H_2O_2.[16–19] A mediator or a catalyst is necessary to provide its electrochemical reaction on the carbon electrode surface. Among various catalysts that have been studied for the detection of H_2O_2 *via* electrochemical methods at carbon-based electrodes, the most studied electrocatalyst is Prussian blue (PB).[20–23] PB, with an empirical formula of $Fe_{4III}[Fe_{II}(CN)_6]_3$, is well known as an artificial peroxidase owing to its high activity and selectivity in reducing H_2O_2 (ref. 24–28) and its ability to operate in physiological solutions as well.[28,29] This distinctive feature makes PB largely used as a catalyst in electrochemical sensors. Moreover, PB can act as a charge transfer mediator owing to its mixed-

[a]*Department of Chemistry, Faculty of Mathematics and Sciences, Universitas Indonesia, Jakarta, Indonesia. E-mail: ivandini.tri@sci.ui.ac.id; isnaini.rahmawati@sci.ui.ac.id*

[b]*Department of Chemistry, Keio University, 3-14-1 Hiyoshi, Yokohama, 223-8522, Japan*

[c]*Department of Chemistry, Faculty of Mathematics and Natural Sciences, University of Padjajaran, Bandung 45363, Indonesia*

[d]*Department of Chemistry, Faculty of Mathematics and Natural Sciences, Kampus IPB Dramaga, Bogor 16680, Indonesia*

[e]*Physics Engineering Department, Institut Teknologi Sepuluh Nopember, Surabaya 60111, Indonesia*

† Electronic supplementary information (ESI) available. See DOI: https://doi.org/10.1039/d4ay02175d

valent iron cyanide.[29] PB-modified electrodes have been largely used in electrochemical sensing of H_2O_2 with the electrodeposition of PB being the commonly used technique to prepare the PB-modified electrode surface.[28,29]

Meanwhile, another method based on an electrochemical technique largely developed for the detection of H_2O_2 is electrochemiluminescence (ECL). ECL is generated from a redox reaction of highly reactive species on the electrode surface when a potential is applied with the generation of an excited state that emits light.[30–32] Besides, because the excitation of light is not needed in ECL, this method exhibits nearly zero background.[33] Moreover, ECL possesses the excellence of electrochemical techniques, such as fast measurements, simple operation processes as well as good selectivity and sensitivity.[30,31] The analytical applications of ECL are mainly performed through a co-reactant pathway in a solution containing luminophore or emitter. It has been reported that the use of H_2O_2 as a co-reactant in ECL systems at BDD electrodes with luminol as a luminophore enhances the ECL signal of luminol due to the radical H_2O_2 helping luminol to undergo an excited state and eventually emits luminescence.[33] The high resistance toward extreme potentials is often required to promote co-reactants to form the intermediate species for ECL measurements.[34–37] Accordingly, this phenomenon was studied to provide the detection of hypochlorite based on luminol ECL at BDD electrodes.[38]

In this work, the detection of H_2O_2 at BDD electrodes was studied using both electrocatalysis by PB and luminol ECL, and a comparison of these two sensing methods is provided.

Experimental

Materials

Experiments were carried out in Milli-Q water (18.2 MΩ cm at 25 °C). Potassium ferricyanide ($K_3Fe(CN)_6$), iron(III) chloride ($FeCl_3$), hydrochloric acid (HCl), potassium chloride (KCl) and 30% hydrogen peroxide (H_2O_2) were purchased from Sigma-Aldrich. Luminol, methane, and trimethoxy borane were obtained from the Tokyo Chemical Industry. Phosphate buffer saline (PBS) pH 7.4 was used as a supporting electrolyte, except otherwise stated. All the chemicals were of analytical grade and used as received.

BDD electrode preparation

The BDD films were prepared on the surface of a silicon wafer (Si 111) using a microwave plasma-assisted chemical vapour deposition system (Model AX-5400, CORNES Technology Corp). As the sources of carbon and boron, methane and trimethoxy borane were used, respectively, with a boron-to-carbon ratio of 1%.[12] The quality of BDD films was confirmed by Raman spectroscopy (Acton SP 2500 Princeton Instruments, with a 532 nm laser) showing a sharp sp^3 peak at 1333 cm^{-1} and scanning electronic microscope (JCM-6000, JEOL) images showed that the polycrystalline films had an average grain size of 5 μm (Fig. S1†). These films were used to replace the working electrodes of screen-printed carbon electrodes (SPCE, DropSens 150, Metrohm). The SPCEs ($d = 0.3$ cm) consist of platinum and silver as counter and quasi-reference electrodes, respectively. Prior to use, a pre-treatment on the BDD electrode surface was performed by a cathodic reduction and anodic oxidation at −3.5 V and +3.5 V, respectively, in 0.1 M $NaClO_4$ solution for 10 min each.

Prussian blue electrodeposition on BDD

The PB-modified BDD (PB-BDD) was prepared by electrochemical deposition of PB on the working electrode of the BDD-SPCE. The deposition was carried out using cyclic voltammetry (CV) from a potential of 0.75 V to 0.4 V at a scan rate of 20 mV s^{-1} for 6 cycles.[29] The electrolyte contained 5 mM $K_3[Fe(CN)_6]$ and 5 mM $FeCl_3$ in 0.1 M KCl and 0.1 M HCl, respectively, to prevent the hydrolysis of ferric ions and to achieve regular and stable polycrystalline films. The PB-BDD was characterized by CV using 0.1 M KCl in 0.1 M HCl from potentials of −0.4 V to 1 V.

Electrochemical and ECL detection instrumentation

All electrochemical and ECL measurements were performed using the Autolab PGSTAT204 electrochemical workstation (Metrohm) at room temperature in phosphate buffer solution (PBS) pH 7.4 to simulate the physiological conditions. Meanwhile, the ECL intensity was collected as the same as in previous research in a dark box by using a Photosensor Module (H11902-20) set at a 1 cm distance above the electrochemical cell.[38] The voltage of 800 mV, triggered by the potentiostat, was applied at the photomultiplier tube (PMT) for the direct acquisition of the ECL signals. All measurements were carried out in 3 repetitions. The schematic of the ECL system is provided in the ESI, S2.†

Detection of H_2O_2

ECL detection of H_2O_2 was carried out by step chronoamperometry using BDD in 0.1 M PBS containing 0.5 mM luminol and various concentrations of H_2O_2. A potential of 0 V was applied for 2 s, and then the optimum potential was applied for 10 s. Electrochemical detection of H_2O_2 was performed by using PB-BDD by chronoamperometry at the optimum potential of 0.2 V for 90 s in 0.1 M PBS solution, current sampled at 30 s.

Results and discussion

Cyclic voltammetry was used to study the ECL behaviour of luminol by using the BDD electrode in the absence and the presence of H_2O_2 (Fig. 1). The ECL of luminol has been previously reported; however, these results are necessary to assess the quality of our electrodes.

A typical ECL peak of luminol was observed at a starting potential of +0.3 V, and the presence of H_2O_2 increases the ECL intensity by approximately eight times. The enhancement is ascribed to the reaction of the oxidised luminol and H_2O_2 in alkaline conditions, where luminol forms luminol radical ($L^{\bullet}$) and H_2O_2 forms superoxide radical anion ($O_2^{\bullet -}$); those radicals further react in a catalytic reaction, which leads to higher

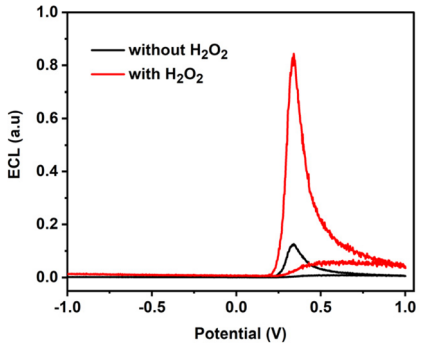

Fig. 1 ECL signal by cyclic voltammetry of 0.5 mM luminol in 0.1 M PBS (pH 7.4) in the absence (black line) and in the presence (red line) of 10 mM H_2O_2, scan rate 0.1 V s^{-1}. WE: BDD.

$$L \rightarrow L^{\bullet+} + e^- \quad (1.1)$$

$$L^{\bullet+} \rightarrow L^{\bullet} + H^+ \quad (1.2)$$

$$H_2O_2 \rightleftharpoons HO_2^- + H^+ \rightarrow HO_2^{\bullet} \quad (1.3)$$

$$HO_2^{\bullet} \rightleftharpoons O_2^{\bullet-} + H^+ \quad (1.4)$$

$$L^{\bullet} + O_2^{\bullet-} \rightarrow 3AP^* \quad (1.5)$$

$$3AP^* \rightarrow 3AP + h\nu_{ECL} \quad (1.6)$$

Scheme 1 Simplified ECL mechanism of luminol (L) and hydrogen peroxide, with emission from 3AP (3-aminophthalate dianion) excited state.

production of the 3-aminophthalate dianion excited state (Scheme 1).[39,40]

For practical applications in the monitoring of H_2O_2 concentration, chronoamperometry is more suitable than cyclic voltammetry, therefore, investigation for the optimum potential by the highest ECL signal generation was measured. Fig. 2 shows the ECL signals at various potentials between +0.3 V and +0.6 V, the potential range of the ECL peak by cyclic voltammetry, where +0.5 V results in the highest signal. Accordingly, this potential was selected for the following experiments.

The luminol ECL response with H_2O_2 was compared against the electrocatalytic reduction of H_2O_2 on Prussian Blue. PB electrocatalyst was electrodeposited on a BDD electrode, namely PB-BDD, in a solution containing hexacyanoferrate(III) and iron(III) chloride. The reaction between iron(III) cations and hexacyanoferrate(II) anions form a highly reactive complex of ferric ferricyanide, or Prussian green (PG). An acidic supporting electrolyte was used to prevent the hydrolysis of ferric ions and to achieve regular and stable polycrystalline films. The reduced PG reacts with free iron(III) cations in the solution and forms insoluble PB according to the following reaction mechanism (eqn (2)–(4)).[41]

$$Fe^{3+} + Fe(CN)_6^{3-} \rightarrow Fe^{III}Fe^{III}(CN)_6 \quad (2)$$

$$Fe^{III}Fe^{III}(CN)_6 + e^- \rightarrow Fe^{II}Fe^{III}(CN)_6^- \quad (3)$$

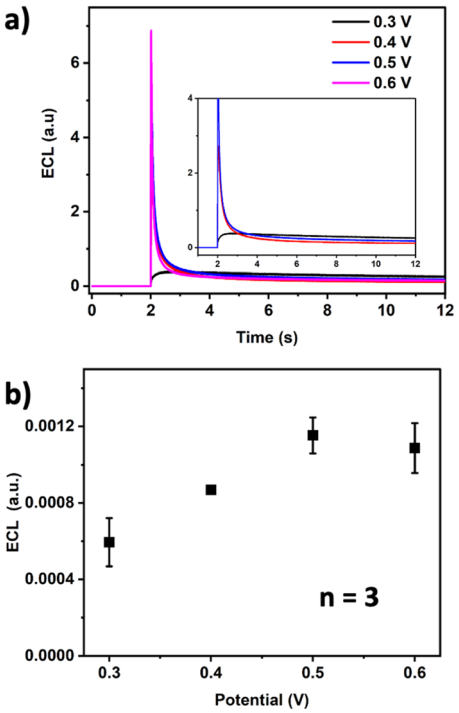

Fig. 2 (a) ECL by chronoamperometry of 0.5 mM luminol in 0.1 M PBS (pH 7.4) in the presence of 10 μM H_2O_2 at different potentials; (b) integrated ECL signals *vs.* applied potential. WE: BDD.

$$3Fe^{II}Fe^{III}(CN)_6^- + Fe^{3+} \rightarrow Fe_4^{III}[Fe^{II}(CN)_6]_3 \quad (4)$$

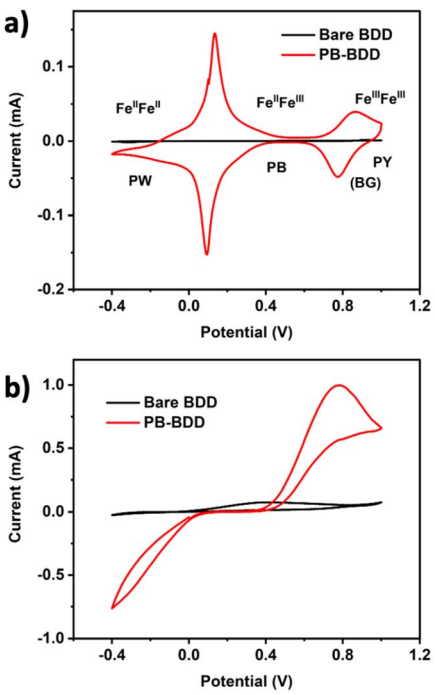

Fig. 3 Cyclic voltammetry of solutions containing (a) 0.1 M KCl and 0.1 M HCl and (b) PBS (pH 71.4) containing 100 mM H_2O_2. WE: bare BDD (black line) and PB-BDD (red line). Scan rate 0.1 V s^{-1}.

Characterization was performed by cyclic voltammetry of PB-BDD electrodes in a solution containing 0.1 M KCl and 0.1 M HCl. Two sets of redox peaks were observed (Fig. 3a), where the first peak at around +0.12 V corresponds to the PB/PW (Prussian white) redox reaction, while the second couple at higher potentials (around +0.9 V) is related to PB to Prussian Yellow (PY) *via* the mixed-valence form of PG, also called Berlin Green (BG).[10,42,43] The sharp couple peaks of PB/PW indicate a regular structure of PB with a homogeneous distribution of charge transfer rates throughout the deposited layer.[29]

Cyclic voltammetry in the presence of H_2O_2 was conducted on PBS at pH 7.4, which is known as the physiological pH, in comparison with the bare BDD electrode (Fig. 3b). Significant currents for both oxidation and reduction were observed at PB-BDD, while there was no relevant current response at the bare BDD.

In the peak observed at a positive potential, Fe undergoes oxidation from Fe^{II} as $Fe^{III}[Fe^{II}(CN)_6]^-$ (PB) to Fe^{III} as $Fe^{III}[Fe^{III}(CN)_6]$ (PY).[44,45]

Further electrocatalysis of H_2O_2 was performed at negative potentials as PB is known as a superior electrocatalyst for the reduction of H_2O_2, according to the reaction in eqn (5).[46,47]

$$Fe_4^{II}K_4[Fe^{II}(CN)_6]_{3(PW)} + 2H_2O_2 \rightarrow Fe_4^{III}[Fe^{II}(CN)_6]_{3(PB)} + 4OH^- + 4K^+ \quad (5)$$

Chronoamperometry measurements at various potentials between −0.1 V to −0.4 V were conducted in a solution containing 10 mM H_2O_2 with the PB-BDD electrode (Fig. 4). The highest current response was observed at −0.2 V. This result confirms the potential of the maximum peak of the cyclic voltammogram of PB/PW redox reactions, which was reported at around −0.1 V to −0.2 V.[28] Accordingly, the potential −0.2 V was used for further analysis.

For potential applications in a biosensor, signal stability for both methods was studied at their optimum potential in PBS at pH 7.4 containing 100 μM H_2O_2 (Fig. 5). Luminol ECL signal at bare BDD was stable for 10 measurements as the ECL intensity showed an RSD of 4.8%. BDD is well-known for its chemical stability, which can prevent surface fouling, therefore retaining good electrochemical response under continuous measurements. The stability of the BDD surface is due to sp^3 carbon hybridization, which contributes to the very weak adsorption properties and makes BDD an ideal non-active electrode.

On the contrary, the reduction current at the PB-BDD electrode significantly decreases by about 30% after 10 measurements. The probable reason of the progressive loss of catalytic activity is the leaching of PB by the reaction with hydroxide ions, which are produced from the reaction with H_2O_2 according to the reaction in eqn (6),[44] although the phosphate electrolyte, which contains KCl is known to stabilize the PB film.

$$Fe_4^{III}[Fe^{II}(CN)_6]_3 + 12OH^- \rightarrow 4Fe(OH)_3 + 3[Fe^{II}(CN)_6]^{4-} \quad (6)$$

The loss of PB from the BDD electrode surface was also confirmed by cyclic voltammetry of the PB-BDD after the stability test (Fig. 5b, inset), which showed a lower current for PB/PG, in particular for the redox peak of PW/PB, which plays a pivotal role in the reduction of H_2O_2.

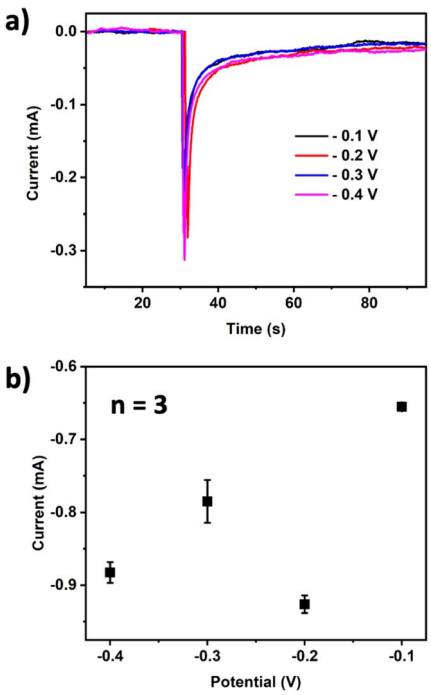

Fig. 4 (a) Chronoamperometry of 10 mM H_2O_2 in 0.1 M PBS (pH 7.4) at various potentials; (b) current response *vs.* the applied potentials. WE: PB-BDD.

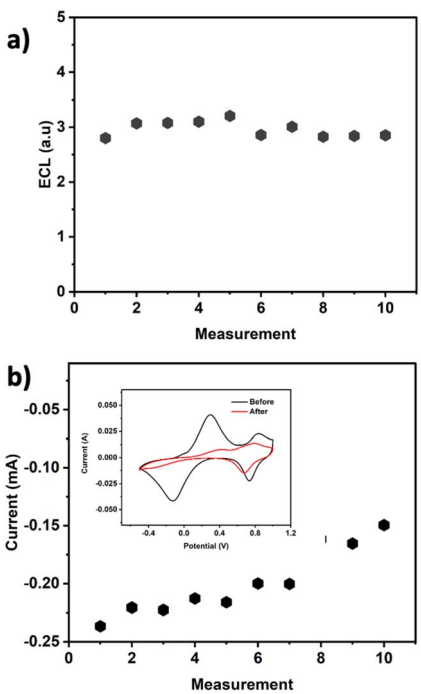

Fig. 5 Stability of the signal responses of PBS at pH 7.4 containing 100 μM H_2O_2 performed with (a) luminol ECL at single unmodified BDD electrodes, and (b) electrocatalyst at PB-BDD.

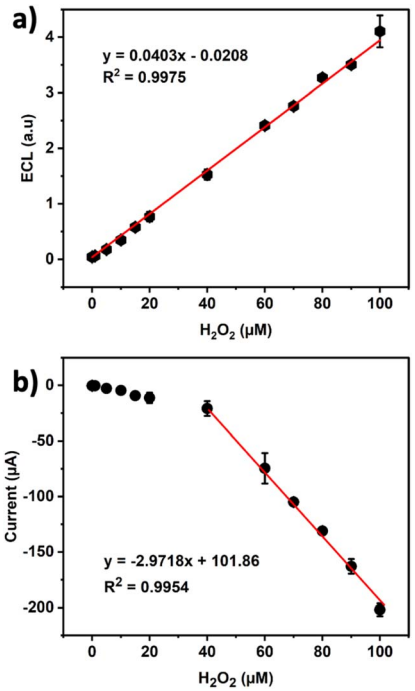

Fig. 6 Calibration curve of (a) chronoamperometry ECL of luminol and (b) electroreduction by PB of various concentrations of H_2O_2 at optimum potential. Error bars indicate standard deviation from triplicate measurements.

The quantitative detection of H_2O_2 was performed using both analytical methods (Fig. 6), where response was found to be proportional with the H_2O_2 concentrations. The linear range of luminol ECL was from 0 to 100 μM ($R^2 = 0.9975$) with an estimated limit of detection (LOD, S/N = 3) of 2.59 μM (Fig. 6a). In the case of PB-BDD electrocatalyst, the linear range was from 40 to 100 μM ($R^2 = 0.9954$) with an estimated LOD of 4.92 μM. In particular, our PB-BDD had a sensitivity of about 110 times (23 A cm^{-2} M^{-1}) higher than those previously reported for PB on BDD (0.21 A cm^{-2} M^{-1}).[28]

The analytical performances of both methods have been compared in Table 1. BDD shows a better detection limit using PB as a catalyst, particularly for low H_2O_2 concentration measurements compared with other electrodes.[20,21] However, electrocatalyst Pt has better performance than PB at the BDD electrode.[17] The developed ECL methods are favourable among other reported sensors and mostly have lower limit detection than normal electrochemistry.[16,19–21,23] However, previous work reported an ECL method using glassy carbon modified with quantum dots, graphene, and gold nanoparticles that showed better performance.[22] This is because an unmodified BDD electrode was used in this work, while that research used modified electrodes for better catalytic performance.[22]

Several potential interferences were studied to investigate the selectivity of the developed sensing methods. Both proposed methods have good selectivity towards H_2O_2 and not being affected by interfering species, although luminol ECL was slightly enhanced by the presence of sulphate (Fig. 7b), however, the possible reasons are still unclear.

The final comparison of the two sensing methods was assessed on the detection of hydrogen peroxide for a complex

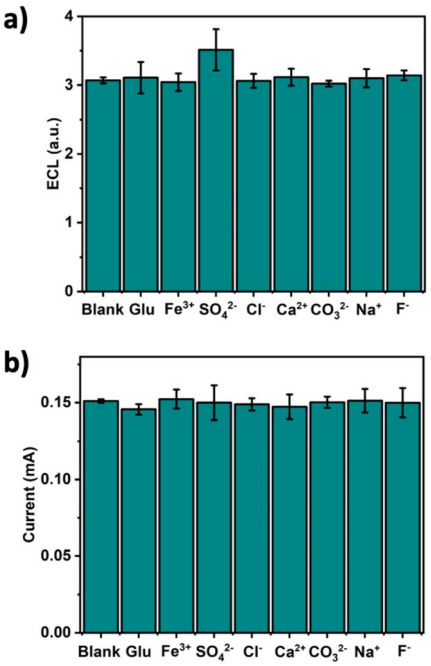

Fig. 7 Evaluation of selectivity for H_2O_2 100 μM determination on the (a) luminol ECL and (b) electroreduction by PB in the presence of possible interferences compounds at 100 μM. Error bars indicate standard deviation from triplicate measurements.

Table 1 Comparison of the current work against other literature studies of various detection methods for the measurements of H_2O_2

Electrode	Detection method	Linear range (μM)	LOD (μM)
HRP-nano-undoped BDD[16]	Colorimetry	0–40000	100
Pt BDD[18]	CV	0.05–20000	0.1
Hemepeptide-peroxidase-BDD[19]	CA	0.1–1000	10^5
PB-fCNT/GC[20]	CA	50–800	15
PB nanocubes/GO[21]	CA	0–150	40
CdSeQDs/GO-Au/GCE[22]	ECL	0.5–500	0.5
G/rGO/polyHm[23]	CV	9.9–50	8.86
PB-BDD[This work]	CA	40–100	4.92
BDD[This work]	ECL	0–100	2.59

Table 2 Determination of H_2O_2 in toothpaste sample using proposed methods. Error represents the standard deviation ($n = 3$)

	Found (μM)		Recovery (%)	
Spiked (μM)	ECL	PB	ECL	PB
20	23.18 ± 0.01	37.68 ± 0.80	111	155
40	41.77 ± 0.02	41.06 ± 0.93	104	98
60	62.87 ± 0.03	59.41 ± 0.59	105	94

matrix, and in this case, toothpaste was chosen as the real sample. The recovery performance was evaluated by matrix spiking of different H_2O_2 concentrations (Table 2). The results showed a recovery of H_2O_2 between 104 to 111% and 94 to 156% for ECL and PB, respectively. Although comparable results could be achieved, a very high recovery percentage (155.27%) was observed when spiking 20 μM using the PB electrocatalyst method, probably due to the interference from components in the toothpaste. Consequently, it can be concluded that although both sensing strategies are acceptable for practical applications, the ECL method provided a more accurate response.

Conclusions

Two different electrochemical methods were successfully compared for the detection of H_2O_2, namely luminol ECL and electroreduction by Prussian blue catalyst, both used a boron-doped diamond electrode. Luminol ECL showed a lower detection limit with an LOD of 2.59 μM compared to 4.92 μM for Prussian blue. A comparable selectivity of the luminol ECL and PB-BDD electrochemical current was shown in the presence of glucose as well as Fe^{3+} and Cl^- ions. Nevertheless, an increase in the ECL signal was measured in the presence of sulphate. Both methods detected H_2O_2 in the toothpaste matrix, although better accuracy of luminol ECL than Prussian blue was found at lower H_2O_2 concentration. These results indicate that the developed sensor could potentially be used as a cholesterol sensor with cholesterol oxidase as the recognition element. This is because the cholesterol concentration will be proportional to the H_2O_2 detected.

Data availability

The datasets supporting this article have been uploaded as part of the ESI.†

Author contributions

Isnaini Rahmawati, Irkham: investigation, data curation, formal analysis, visualization, writing – original draft. Wulan Tri Wahyuni, Ruri Agung Wahyuono, Andrea Fiorani: conceptualization, supervision, formal analysis, writing – review & editing. Yasuaki Einaga: validation. Tribidasari A. Ivandini: conceptualization, supervision, validation, funding acquisition, writing – review & editing.

Conflicts of interest

There are no conflicts to declare.

Acknowledgements

The authors would like to sincerely thank the Riset Kolaborasi Indonesia Grant No. NKB-767/UN2.RST/HKP.05.00/2024.

References

1 Y. Yu, M. Pan, J. Peng, D. Hu, Y. Hao and Z. Qian, *Chin. Chem. Lett.*, 2022, **33**(9), 4133–4145.
2 W. Chen, S. Cai, Q. Ren, W. Wen and Y. Zhao, *Analyst*, 2012, **137**, 49.
3 R. Gaikwad, P. R. Thangaraj and A. K. Sen, *Sci. Rep.*, 2021, **11**, 2960.
4 H. Tavakkoli, M. Akhond, G. A. Ghorbankhani and G. Absalan, *Microchim. Acta*, 2020, **187**, 105.
5 C. Wu, G. Xia, J. Sun and R. Song, *RSC Adv.*, 2015, **5**, 97648.
6 N. V. Klassen, D. Marchington and H. C. E. McGowan, *Anal. Chem.*, 1994, **66**(18), 2921.
7 M. H. Irani-nezhad, A. Khataee, J. Hassanzadeh and Y. Orooji, *Molecules*, 2019, **24**(4), 689.
8 E. Ito, S. Watabe, M. Morikawa, H. Kodama, R. Okada and T. Miura, *Methods Enzymol.*, 2013, **526**, 135.
9 H. Shamkhalichenar and J. Choi, *J. Electrochem. Soc.*, 2020, **167**, 037531.
10 K. Sakanoue, A. Fiorani, I. Irkham and Y. Einaga, *ACS Appl. Electron. Mater.*, 2021, **3**(9), 4180.
11 I. Irkham, R. R. Raishaqy, T. A. Ivandini, A. Fiorani and Y. Einaga, *Anal. Chem.*, 2021, **93**, 2336.
12 T. A. Ivandini, T. Watanabe, T. Matsui, Y. Ootani, S. Iizuka, R. Toyoshima, H. Kodama, H. Kondoh, Y. Tateyama and Y. Einaga, *J. Phys. Chem. C*, 2019, **123**, 5336–5344.
13 T. A. Ivandini, W. P. Wicaksono, E. Saepudin, B. Rismetov and Y. Einaga, *Talanta*, 2015, **134**, 136–143.
14 K. Asai, T. A. Ivandini, M. M. Falah and Y. Einaga, *Electroanalysis*, 2016, **28**, 177.
15 M. C. Granger, J. Xu, J. W. Strojek and G. M. Swain, *Anal. Chim. Acta*, 1999, **397**, 145.
16 Q. Wang, *et al.*, *Langmuir*, 2012, **28**, 587–592.
17 T. A. Ivandini, R. Sato, Y. Makide, A. Fujishima and Y. Einaga, *Chem. Lett.*, 2004, **33**(10), 1330–1331.
18 B. Rismetov, T. A. Ivandini, E. Saepudin and Y. Einaga, *Diamond Relat. Mater.*, 2014, **48**, 88–95.
19 T. Tatsuma, H. Mori and A. Fujishima, *Anal. Chem.*, 2000, **72**(13), 2919–2924.
20 L. A. Guerrero, *et al.*, *Nanomaterials*, 2020, **10**(1), 64.
21 L. Cao, Y. Liu, B. Zhang and L. Lu, *ACS Appl. Mater. Interfaces*, 2010, **2**(8), 2339–2346.
22 Y. X. Hu, C. M. Chen, Y. Liu, S. Wang, Z. Y. Guo and Y. F. Hu, *J. Electroanal. Chem.*, 2018, **815**, 61–67.
23 A. R. Deac, L. M. Muresan, L. C. Cotet, L. Baia and G. L. Turdean, *J. Electroanal. Chem.*, 2017, **802**, 40–47.
24 A. A. Karyakin, *Curr. Opin. Electrochem.*, 2017, **5**, 92–98.

25 D. V. Vokhmyanina, K. D. Andreeva, M. A. Komkova, E. E. Karyakina and A. A. Karyakin, *Talanta*, 2020, **208**, 120393.
26 M. A. Komkova, O. A. Ibragimova, E. E. Karyakina and A. A. Karyakin, *J. Phys. Chem. Lett.*, 2021, **12**, 171–176.
27 E. V. Karpova, E. V. Shcherbacheva, M. A. Komkova, A. A. Eliseev and A. A. Karyakin, *J. Phys. Chem. Lett.*, 2021, **12**, 5547–5551.
28 M. A. Komkova, A. Pasquarelli, E. A. Andreev, A. A. Galushin and A. A. Karyakin, *Electrochim. Acta*, 2020, **339**, 135924.
29 A. M. Farah, C. Billing, C. W. Dikio, A. N. Dibofori-Orji, O. O. Oyedeji, D. Wankasi, F. M. Mtunzi and E. D. Dikio, *Int. J. Electrochem. Sci.*, 2013, **8**, 12132.
30 W. Miao, J. Choi and A. J. Bard, *J. Am. Chem. Soc.*, 2002, **124**, 14478.
31 M. M. Richter, *Chem. Rev.*, 2004, **104**, 3003.
32 K. Muzyka, *Biosens. Bioelectron.*, 2014, **54**, 393.
33 X. Zu and T. Gao, *Nano-Inspired Biosensors for Protein Assay with Clinical Applications: Chapter 10 – Spectrometry*, 2019, p. 237.
34 S. Garcia-Segura, F. Centella and E. Brillas, *J. Phys. Chem. C*, 2012, **116**(29), 15500.
35 I. Rahmawati, I. Irkham, R. Wibowo, J. Gunlazuardi, Y. Einaga and T. A. Ivandini, *Indones. J. Chem.*, 2021, **21**, 1599.
36 I. Irkham, R. R. Raishaqy, T. A. Ivandini, A. Fiorani and Y. Einaga, *Anal. Chem.*, 2021, **93**, 2336.
37 I. Irkham, A. Fiorani, G. Valenti, N. Kamoshida, F. Paolucci and Y. Einaga, *J. Am. Chem. Soc.*, 2020, **142**(3), 1518.
38 I. Rahmawati, E. Saepudin, A. Fiorani and T. A. Ivandini, *Analyst*, 2022, **147**(12), 2696–2702.
39 H. Li, H. Zhou, T. Zhang, Z. Zhang, G. Zhao and C. Wang, *ACS Sustainable Chem. Eng.*, 2022, **10**(31), 10361–10368.
40 H. Li, G. Zhao, Y. Yang, N. Sojic and C. Wang, *Sens. Actuators, B*, 2024, **403**, 135186.
41 H. Akbari Khorami, P. Wild, A. G. Brolo and N. Djilali, *Sens. Actuators, B*, 2016, **237**, 113.
42 R. Koncki, *Crit. Rev. Anal. Chem.*, 2002, **32**, 79.
43 Y. Matos-Peralta and M. Antuch, *J. Electrochem. Soc.*, 2020, **167**, 037510.
44 D. J. Schmidt, *et al.*, *ACS Nano*, 2009, **3**(8), 2207–2216.
45 K. Y. Goud, *et al.*, *Mikrochim. Acta*, 2019, **186**(12), 81.
46 J. Yang, M. Lin, M. S. Cho and Y. Lee, *Microchim. Acta*, 2015, **182**, 1089.
47 J. M. Noël, J. Médard, C. Combellas and F. Kanoufi, *ChemElectroChem*, 2016, **3**, 1178.

